The phosphatase PTEN-mediated control of PI-3 kinase in Tregs cells maintains homeostasis and lineage stability

Published in final edited form as:
Nat Immunol. 2015 February ; 16(2): 188–196. doi:10.1038/ni.3077.

The phosphatase PTEN-mediated control of PI-3 kinase in T_{regs} cells maintains homeostasis and lineage stability

Alexandria Huynh[1,2], **Michel DuPage**[3], **Bhavana Priyadharshini**[2], **Peter T. Sage**[4], **Jason Quiros**[3], **Christopher M. Borges**[1,2], **Natavudh Townamchai**[5], **Valerie A. Gerriets**[6], **Jeffrey C. Rathmell**[6], **Arlene H. Sharpe**[4], **Jeffrey A. Bluestone**[3], and **Laurence A. Turka**[1,2]

[1]Division of Medical Sciences, Harvard Medical School, Boston, MA [2]Center for Transplantation Sciences, Department of Surgery, Massachusetts General Hospital, Boston, MA [3]Diabetes Center and the Department of Medicine, University of California - San Francisco, San Francisco, CA [4]Division of Immunology, Department of Microbiology, Harvard Medical School, Boston, MA [5]Division of Nephrology, Department of Medicine, Chulalongkorn University and King Chulalongkorn Memorial Hospital, Bangkok, Thailand [6]Department of Pharmacology and Cancer Biology, Duke University Medical Center, Durham, NC

Abstract

$Foxp3^+$ regulatory T cells (T_{regs}) are required for immune homeostasis. One notable distinction between conventional T cells (T_{conv}) and T_{regs} is differential phosphatidylinositol 3-kinase (PI3K) activity: only T_{conv} downregulate PTEN, the primary negative regulator of PI3K, upon activation. Here, we show that control of PI3K in T_{regs} is essential for lineage homeostasis and stability. Mice lacking *Pten* in T_{regs} developed an autoimmune-lymphoproliferative disease characterized by excessive T_H1 responses and B cell activation. Diminished control of PI3K activity in T_{regs} led to reduced CD25 expression, accumulation of $Foxp3^+CD25^-$ cells and ultimately, loss of Foxp3 expression in these cells. Collectively, these data demonstrate that control of PI3K signaling by PTEN in T_{regs} is critical to maintain their homeostasis, function and stability.

Regulatory T cells (T_{regs}) defined by expression of the transcription factor Foxp3 are required for normal immune homeostasis. Mutation of the *Foxp3* gene in mouse and human leads to the *scurfy* phenotype and IPEX disease, respectively, both characterized by the lack of functional T_{regs}, autoimmunity, and systemic polyclonal lymphoproliferation[1, 2]. This central role of T_{regs} in immune tolerance has led to a focus on defining the signals that govern T_{reg} generation, function and stability[3]. Critical among these signals are those

Correspondence: Laurence A. Turka, Center for Transplantation Sciences, MGH-East, Bldg. 149-9019, 13th Street Boston, MA 02129 Phone: 617 724-7740; Fax: 617-726-6925, lturka@partners.org.

Author contributions

A.H., M.D., B.P., P.T.S., J.Q., N.T. and V.A.G. designed and performed experiments; C.M.B., J.C.R., and A.H.S. designed experiments; A.H., M.D., J.A.B. and L.A.T. designed the study; A.H. and L.A.T. wrote the manuscript with assistance from M.D. and J.A.B.

Competing financial Interests

The authors declare a competing financial interest. For information see, **xxxxxxxxxxx**.

Accession codes: GSE60057

delivered by the interleukin 2 receptor (IL-2R), as enhancement of IL-2R signaling dramatically expands T_{regs} *in vivo*[4]. Among the signals activated via the IL-2R, phosphorylation of STAT5 appears to be particular important for T_{reg} maintenance and expansion[5].

In addition to activation of STAT5, IL-2 also initiates signaling through phosphatidylinositol 3-kinase (PI3K), which can be activated as well via the TCR or CD28[6, 7]. The primary negative regulator of PI3K is phosphatase and tensin homolog on chromosome 10 (PTEN), a lipid phosphatase, which catalyzes the reverse reaction of PI3K[8]. Demonstrating the importance of PI3K regulation in immune homeostasis, animals harboring one inactive PTEN allele, develop systemic autoimmunity, which has been attributed in part to defects in thymic negative selection, as well as in Fas-mediated and activation-induced cell death in potential effector T cells. While T cell-specific PTEN deficiency leads to a lethal $CD4^+$ T cell lymphoma of thymic origin[7, 9, 10], when lymphoma development is prevented by early thymectomy, systemic autoimmunity is observed, indicating that targeting PTEN in T cells is sufficient to disturb self-tolerance.

We and others, have previously shown that regulatory T cells, but not effector T cells, maintain high amounts of PTEN expression, thus preventing the downstream activation of PI3K targets following IL-2 stimulation, while allowing further JAK-STAT signaling[11, 12]. Indeed, control of PTEN via the scaffold protein Disc large homolog 1 is critical for human T_{reg} function *in vitro*[13]. This suggests that T_{regs} require a mechanism of PI3K control distinct from effector T cells.

Consistent with this notion, PI3K signaling inhibits *in vitro* T_{reg} differentiation and homeostasis, while rapamycin promotes T_{reg} proliferation and accumulation in the periphery[14–18]. Conversely, pharmacological inhibition of PI3K signaling enhances *in vitro* T_{reg} differentiation[14, 19] and expression of a constitutively active Akt allele in T_{regs} leads to an overall dampening of the T_{reg} gene signature, including reduced expression of *Foxp3*, *Il2ra* (CD25), and *Ctla4*[16].

To define the cell-intrinsic function of the PI3K pathway in T_{reg} homeostasis, we generated mice lacking expression of PTEN specifically within the $Foxp3^+$ population, termed *Pten*-ΔT_{reg} mice. Disruption of PTEN did not result in catastrophic decreases in $Foxp3^+$ T_{regs}; in fact, there was an increase in the $CD25^-$ subset of $Foxp3^+$ cells. However, despite the continued presence of the $Foxp3^+$ T_{reg} population, *Pten*-ΔT_{reg} mice developed a systemic polyclonal lymphoproliferative disease and renal failure. Female mice heterozygous for *Foxp3*-Cre were initially healthy, but over time their wild-type T_{reg} compartment was replaced by PTEN-deficient T_{regs}, and they ultimately succumbed to disease. Further studies revealed that loss of PTEN was associated with disruptions in cellular metabolism and energy utilization. Finally, we found that elevation of PI3K signaling in PTEN-deficient regulatory T cells led directly to the successive loss of CD25 followed by Foxp3, and the emergence of ‘ex’-Foxp3 cells (i.e., cells which were once $Foxp3^+$ but appear to have permanently lost Foxp3 expression). Together, these data show that control of PI3K signaling via PTEN is required to maintain T_{reg} homeostasis, function and Foxp3 expression.

Results

Generation of *Pten*-ΔT_{reg} mice

Pten$^{fl/fl}$ and *Foxp3-Cre* mice were crossed to generate *Pten*-ΔT_{reg} mice, which lack PTEN expression specifically in the Foxp3$^+$ population of cells (Fig. 1a). Unlike animals lacking PTEN in all T cells[19], *Pten*-ΔT_{reg} mice developed an expanded T_{reg} population in multiple tissues at young ages, while maintaining normal T cell development (Fig. 1b, Supplementary Fig. 1a). Though these PTEN-deficient T_{regs} were generally phenotypically normal (Supplementary Fig. 1b), they expressed substantially lower amounts of the high-affinity IL-2 receptor subunit, CD25, than did control *Pten*$^{+/+}$ *Foxp3*-Cre T_{regs} (Fig. 1c). To exclude the possibility that downregulation of CD25 was a consequence of unappreciated developmental abnormalities, we used a tamoxifen-inducible system to delete PTEN *in vitro* from pre-existing Foxp3$^+$ cells. Deletion of PTEN led to a marked reduction in CD25 expression (Fig. 1d), thus demonstrating that PTEN deletion is sufficient to downregulate CD25 in otherwise normal T_{regs}.

Development of disease in *Pten*-ΔT_{reg} mice

Despite their enlarged T_{reg} compartment, *Pten*-ΔT_{reg} mice developed peripheral lymphoproliferative disease (defined as grossly visible lymphadenopathy) with age (Fig. 2a) that appeared as early as 12 weeks of age, and by 28 weeks of age affected approximately 80% of animals. While lymphoproliferation affected secondary lymphoid tissue, thymic cellularity was not increased, most likely due to the affects of autoimmunity (see below) with B cell infiltration of the thymus (data not shown). Interestingly, the lymphocyte compartments of diseased *Pten*-ΔT_{reg} mice were notable for a further increase in the population of Foxp3$^+$CD25$^-$ cells compared to healthy mice, and a large expansion of activated CD4$^+$CD44^{hi}CD62L^{lo} T cells (Fig. 2b). Expanded CD44^{hi}CD62L^{lo} cells were seen within the T_{reg} compartment itself, in association with elevated ICOS expression (Fig. 2c).

We observed a large accumulation of germinal center B cells in both healthy and diseased *Pten*-ΔT_{reg} mice (Supplementary Fig. 2a), accompanied by high concentrations of serum IgG1, IgG2a/c and IgG2b, and a decrease in IgG3 in diseased mice (Fig. 2d). Consistent with elevations in immunogloblulin concentrations, *Pten*-ΔT_{reg} mice had marked increases in T_{FH} cell numbers (defined as CD4$^+$ICOS$^+$CXCR5$^+$Foxp3$^-$ cells) in the spleen (Supplementary Fig. 2b). Increases in T_{FR} cell numbers were also observed (Supplementary Fig. 2b), consistent with the general increases in T_{reg} cell numbers observed in *Pten*-ΔT_{reg} mice. In addition, when conventional T cells from diseased *Pten*-ΔT_{reg} mice were stimulated *ex vivo*, a large population of IFN-γ producing cells was detected (Fig. 2e). There was no increase in IL-17 production from T cells isolated from either spleen, mesenteric lymph node or colonic lamina propria (Fig. 2e and data not shown). Consistent with this, both T_{regs} and conventional T cells isolated from *Pten*-ΔT_{reg} mice had elevated expression of the chemokine receptor CXCR3, which promotes cell homing to sites of T_H1-type inflammation (Supplementary Fig. 2c)[20]. These data collectively suggest that *Pten*-ΔT_{reg} mice develop a T_H1-type lymphoproliferative disease involving both T and B cells.

Most visceral organs from aged and visibly ill *Pten*-ΔT_{reg} mice had normal gross and histologic appearance (data not shown), with the notable exception of the kidneys (Fig. 2f), which revealed a proliferative glomerulonephritis, interstitial infiltrates and cortical atrophy. This histologic picture was accompanied by elevations in serum concentrations of anti-double stranded DNA antibodies and creatinine (Fig. 2g,h). The rise in serum creatinine concentrations corresponded temporally with the onset of visible lymphadenopathy, indicating that kidney failure and autoimmunity occurred concomitantly. As with secondary lymphoid organs, we found a large population of $Foxp3^+CD25^-$ cells within the diseased kidneys (Supplementary Fig. 2d).

As PTEN deletion in T cells and non-lymphoid cells can lead to malignancy in mice and humans[9, 21], we addressed the possibility that *Pten*-ΔT_{reg} mice had developed malignant disease rather than autoimmunity. One characteristic of autoimmunity in thymectomized *Pten*-ΔT mice is the maintenance of normal TCR Vβ diversity, while PTEN-null T cell malignancies are monoclonal[10]. We found comparable TCR Vβ diversity in both naïve $CD4^+$ cells and T_{reg} isolated from diseased mice, strongly suggesting that the hyperplastic cells were not malignant (Supplementary Fig. 2e). Finally, the expanded population of T cells also predominantly expressed low amounts of CD24 (HSA), in contrast with what is observed in PTEN-deficient T cell malignancies, which, like thymocytes, are $CD24^{hi}$ (Supplementary Fig. 2e)[10, 22]. Thus the expanded population of T cells in *Pten*-ΔT_{reg} mice is a polyclonal non-malignant population.

Defective regulation by PTEN-deficient T_{regs}

As we observed elevated numbers of T_{regs} in *Pten*-ΔT_{reg} mice, we next used BrdU labeling to assess their *in vivo* proliferative capacity. While PTEN-deficient $Foxp3^+CD25^+$ T_{regs} were more proliferative than wild-type controls, BrdU incorporation was highest in the $Foxp3^+CD25^-$ T_{reg} subset (Fig. 3a). Interestingly, these proliferative differences in $Foxp3^+CD25^+$ and $Foxp3^+CD25^-$ cells were seen in both *Pten*-ΔT_{reg} mice as well as wild-type controls (Fig. 3a). To further assess the *in vivo* maintenance of PTEN-deficient T_{regs}, we utilized the X-linked nature of the *Foxp3*-Cre knock-in transgene and bred female $Pten^{fl/fl}$ mice to be heterozygous for *Foxp3*-Cre[23]. Due to random X-inactivation, *Foxp3*-Cre heterozygous females should maintain a 50:50 ratio of Cre^+YFP^+ PTEN-deficient T_{regs}:Cre^-YFP^- PTEN-sufficient wild-type T_{regs}. This was the case in young Cre heterozygous mice, which did not develop activated T cell accumulation at the same time as their *Pten*-ΔT_{reg} counterparts. However, over time, we found that the PTEN-deficient T_{regs} were increased in number relative to wild-type T_{regs} in the blood and lymph nodes of *Foxp3*-Cre heterozygous females (Fig. 3b and data not shown), and this was accompanied by the eventual onset of disease (Fig. 3c,d), presumably due to the loss of wild-type T_{regs}.

From these data, we hypothesized that the lymphoproliferative disease seen in *Pten*-ΔT_{reg} mice could result from three distinct, but non-mutually exclusive processes: PTEN-deficient T_{regs} were unable to perform normal regulatory functions and control effector T cell responses; PTEN deletion caused T_{reg} lineage instability, therefore generating pathogenic PTEN-deficient effector cells; and transient expression of *Foxp3* by non-T_{regs} caused

aberrant excision of PTEN, leading to the generation of pathogenic PTEN-deficient non-T_{regs}.

We first excluded the possibility of transient expression of *Foxp3* in non-T_{regs} leading to Cre-mediated *Pten* excision by assessing *Pten* recombination status at the genomic locus in sorted cell populations from young, healthy *Pten*-ΔT_{reg} mice (Supplementary Fig. 3)[24]. Using primers to specifically detect the deleted *Pten* locus, we found that recombination of *Pten* was only seen in $Foxp3^+$ populations and in neither naïve nor activated T cells, indicating that Cre-mediated *Pten* excision was faithful and confined to the $Foxp3^+$ T_{reg} population.

Next, we used the experimental autoimmune encephalomyelitis (EAE) model to analyze the *in vivo* functional capacity of PTEN-deficient T_{regs}. We found that while the initial onset of disease was similar in *Pten*-ΔT_{reg} and wild-type mice, *Pten*-ΔT_{reg} mice were unable to spontaneously resolve the disease, a process which has previously been shown to be T_{reg} dependent[25]. Notably, progression of symptoms in *Pten*-ΔT_{reg} mice occurred despite the mice maintaining high numbers of $Foxp3^+$ cells in secondary lymphoid organs as well as in the brain itself (Fig. 4a,b), and as would be anticipated, disease severity was accompanied by increased production of IFN-γ and IL-17 by effector T cells (Fig. 4c). Interestingly, however, we found that $Foxp3^+$ cells in *Pten*-ΔT_{reg} mice produced IL-17 to a similar degree as did non-T_{regs} (Fig. 4c), suggesting that these PTEN-deficient T_{regs} might be pathogenic *in vivo*.

The apparent functional defects of PTEN-deficient $Foxp3^+$ cells in our *in vivo* models led to the question of whether these cells were *bona fide* T_{regs}. We performed transcriptional analysis on PTEN-deficient $Foxp3^+CD25^+$ and $Foxp3^+CD25^-$ cells and found that both populations of PTEN-deficient T_{regs} maintained normal expression of Treg signature genes[26] including *Foxp3, Ctla4* and *Nrp1* (Supplementary Fig. 4). Collectively, these data show that *Pten*-ΔT_{reg} mice were unable to resolve the inflammatory insult of EAE, despite the continued presence of high numbers of T_{regs}.

Elevated glycolytic activity in PTEN-deficient T_{regs}

Metabolic programming may dictate T cell fate decisions that occur during differentiation[27]; PI3K activity promotes glycolytic metabolism in various cell types including conventional T cells[28], while in contrast T_{regs} favor oxidative metabolism to meet their energy demands[29]. Strikingly, we observed that T_{regs} from *Pten*-ΔT_{reg} mice had a much higher glucose-stimulated increase in extracellular acidification rate (ECAR – an indirect measurement of glycolysis), compared to wild-type T_{regs} (Fig. 5b). The mitochondrial ATP synthase inhibitor oligomycin did not further increase ECAR but decreased the oxygen consumption rate (OCR – an indicator of mitochondrial respiration), suggesting that maximal glycolytic capacity was reached by the initial addition of glucose in both populations (data not shown). The return of ECAR to basal levels in response to the addition of 2-deoxy-glucose indicates that glucose-stimulated changes in ECAR were due to glycolysis (Fig. 5b). In contrast to this, the ATP coupled respiration and the spare respiratory capacity (SRC) of PTEN-deficient T_{regs} as measured by the OCR, after addition of oligomycin and FCCP respectively was similar to that of wild-type T_{regs} (Fig. 5c). Further, addition of etomoxir, which blocks

mitochondrial fatty acid oxidation, followed by rotenone and antimycin (to block complex-I and complex-III of the electron transport chain respectively) reduced the SRC in both PTEN-deficient T_{regs} and wild-type T_{regs} to a similar degree (Fig. 5c). This overlapping mitochondrial profile between the two populations suggests that mitochondrial function was unimpaired in T_{regs} in the absence of PTEN. Finally, to independently confirm the increase in glycolytic metabolism of *Pten*-ΔT_{reg} cells, we measured their glycolytic rate via assessing the generation of ^3H_2O from [3-^{3}H]-glucose. Consistent with our Seahorse data, we found that *Pten*-ΔT_{reg} cells possessed a higher glycolytic rate than their wild-type counterparts upon activation (Fig. 5d). Together, these findings indicate that PTEN deficiency in T_{regs} renders them hyperglycolytic, a bioenergetic state that could disrupt their homeostasis and cause functional instability.

PTEN-deficient T_{regs} are unstable

While the severity of EAE-related inflammation in *Pten*-ΔT_{reg} mice as well as the ultimate development of autoimmune disease onset in Cre heterozygous females may be a result of an inherent inability of PTEN-deficient T_{regs} to perform normal regulatory function, these data could also indicate compromised stability of PTEN-deficient T_{regs}, particularly during inflammatory settings. One potential marker of T_{reg} instability as a result of PTEN loss would be methylation of the T_{reg}-specific demethylated region (TSDR)[30]. Methylation of the *Foxp3* locus has been associated previously with maintenance of Foxp3 expression and resultant T_{reg} stability[30]. Therefore, we analyzed TSDR methylation in Foxp3$^+$CD25$^+$ and Foxp3$^+$CD25$^-$ cells purified by sorting from wild-type and *Pten*-ΔT_{reg} mice. We observed a moderate reduction of TSDR demethylation in CD25$^+$ PTEN-deficient T_{regs} compared to wild-type CD25$^+$ T_{regs} (Fig. 6). Interestingly, a similar “loss” of demethylation was observed in both populations of Foxp3$^+$CD25$^-$ T_{regs}, which is consistent with lower expression of Foxp3 protein in both wild-type and PTEN-deficient CD25$^-$ T_{regs} ([31–33] and Supplementary Fig. 5).

To more directly evaluate PTEN-deficient T_{reg} stability, sort purified *in vitro*-induced Foxp3$^+$CD25$^+$ T_{regs} were cultured in the presence of IL-2. We observed that PTEN-deficient T_{regs} began to downregulate CD25 expression by 48h, and subsequently lost expression of Foxp3 (Fig. 7a). Blockade of PI3K signals prevented both CD25 and Foxp3 loss, but had no effect on wild-type T_{regs} (Fig. 7a). As loss of CD25 expression preceded loss of Foxp3, the Foxp3$^+$CD25$^-$ phenotype may be an initial, and perhaps inciting, step in T_{reg} destabilization. The fact that neither supplemental IL-2 nor PI3K inhibition alone was able to fully stabilize Foxp3 and CD25 expression (Supplementary Fig. 6a), provides further evidence for the importance of the proper integration and modulation of PI3K and CD25 signals in T_{reg} stability.

As PI3K activation is upstream of both mTORC1 and mTORC2, we assessed the activation of these two arms of the mTOR pathway via the phosphorylation of their downstream targets S6 (mTORC1) and Akt (Serine 473, mTORC2). While PTEN-deficient T_{regs} exhibited enhanced phosphorylation of Akt both at baseline and following TCR/CD28 stimulation, pS6 levels were not increased over control T_{regs} either at rest or after stimulation (Supplementary Fig. 6b), indicating a preferential over-activation of mTORC2.

Similarly, inhibition of Akt (which is activated by PI3K and mTORC2) was more effective than rapamycin, which primarily affects mTORC1, at restoring CD25 expression on PTEN-deficient T_{regs} *in vitro* (Supplementary Fig. 6c).

STAT5 binds to the *Foxp3* promoter, thus regulating its expression and possibly stability[5]. As CD25 downregulation preceded loss of Foxp3 expression *in vitro*, we assessed the downstream phosphorylation of STAT5 within PTEN-deficient $Foxp3^{+}CD25^{+}$ T_{regs}. Importantly, we found brief stimulation with IL-2 induced similar amounts of pSTAT5 in $Foxp3^{+}CD25^{+}$ cells from both *Pten*-ΔT_{reg} mice and wild-type mice, demonstrating that elevated PI3K signaling does not alter the ability of T_{regs} to respond to IL-2 stimulation (Fig. 7b)[11].

As noted above, a deleted *Pten* allele was only detected in $Foxp3^{+}$ cells in young, healthy *Pten*-ΔT_{reg} mice (Supplementary Fig. 3). Thus, we speculated that appearance of the genomic deletion in the $Foxp3^{-}$ population would be suggestive of PTEN-deficient T_{reg} instability. In fact, we found evidence of *Pten* deletion at the genomic level in the activated $CD4^{+}$ $CD44^{hi}CD62L^{lo}Foxp3^{-}$ population of cells in diseased mice (Supplementary Fig. 7), consistent with this hypothesis. To further examine if these PTEN-deleted effector cells did indeed derive from *bona fide* T_{regs}, we took advantage of fate-mapping to assess and quantify the loss of Foxp3 in T_{regs} following deletion of PTEN. *Pten*$^{fl/fl}$ mice were crossed to *Foxp3*$^{eGFP\text{-}Cre\text{-}ERT2}$ Rosa26-YFP mice[34] to generate *Pten*-iΔT_{reg} mice. In these animals, treatment with tamoxifen leads to deletion of PTEN in $Foxp3^{+}$ cells, which are simultaneously "marked" by excision of a stop codon in the ubiquitously expressed Rosa26 locus, allowing the transcription and expression of YFP. While in theory, eGFP can be used as a surrogate for Foxp3 expression, in practice we found that the eGFP signal in the Foxp3 locus was relatively weak compared with the much stronger YFP signal in the Rosa26 locus (data not shown). This, coupled with the known high degree of spectral emission overlap between GFP and YFP, made it simpler to assess Foxp3 expression directly by antibody staining while preserving Rosa26-YFP expression (Supplementary Fig. 8). A population of $Foxp3^{-}$ cells within the YFP^{+} population could be distinguished in the blood of both *Pten*-iΔT_{reg} mice and wild-type *Foxp3*$^{eGFP\text{-}Cre\text{-}ERT2}$ Rosa26-YFP mice (i*Foxp3*-Cre) as early as 1 week after initiation of a 5 day course of tamoxifen (Fig. 8a). Notably, by 10 weeks post-tamoxifen treatment, the percentage of 'ex'-Foxp3 cells in *Pten*-iΔT_{reg} mice was ~30%, i.e., three times higher than that seen in control animals (Fig. 8a). This increase in 'ex'-Foxp3 cells persisted for as long as 18 weeks post-tamoxifen (the last time point at which animals were bled). Confirming data from female *Pten*-ΔT_{reg} mice heterozygous for *Foxp3*-Cre, reduction of CD25 expression was specific for T_{regs} in which PTEN was deleted (Fig. 8b). As 'ex'-Foxp3 cells were observed in both control and *Pten*-iΔT_{reg} mice, we also examined their expression of CD25, and found similar reductions in CD25 expression following loss of Foxp3 in both animals (Fig. 8c). Collectively, these data indicate that PTEN is important for the maintenance of T_{reg} CD25 expression and T_{reg} stability *in vivo*.

Discussion

The data presented in this manuscript, together with another group[35], demonstrate that PTEN-mediated control of PI3K activity is critical for the function and stability of murine

Foxp3$^+$ regulatory T cells. Disruption of PTEN results in reduced CD25 expression, the accumulation of Foxp3$^+$CD25$^-$ cells, and ultimately, the loss of Foxp3 expression. Prior to the discovery and characterization of the Foxp3 transcription factor, high expression of CD25 was used to demarcate T_{regs} from effector T cells. As such, little relevance has been attributed to the small portion of Foxp3$^+$ cells with low CD25 expression, and they have only been assessed in minimal detail compared to canonical Foxp3$^+$CD25$^+$ cells. Here, we have identified a population of Foxp3$^+$CD25$^-$ cells in *Pten*-ΔT_{reg} mice, which appear to be intermediates during the complete destabilization of canonical Foxp3$^+$CD25$^+$ T_{regs}. Accordingly, these Foxp3$^+$CD25$^-$ "T_{reg}" cells displayed a transitional phenotype, where their T_{reg} transcriptional profile was maintained despite a partially methylated Foxp3 TSDR, consistent with their lower Foxp3 protein expression.

We observed nearly normal CD25 expression in newly-generated PTEN-deficient T_{regs} in the thymus, suggesting that the destabilization process occurred after the generation of canonical T_{regs} expressing high levels of CD25. Strikingly, the small population of Foxp3$^+$CD25$^-$ "T_{regs}" present in wild-type mice was seen to have much the same transcriptional profile as their PTEN-deficient counterparts. It is possible that loss of PTEN expression causes proliferation and/or confers a survival advantage upon a normal population of unstable Foxp3$^+$CD25$^-$ cells, which are non-pathogenic in wild-type mice either due to proper regulation by Foxp3$^+$CD25$^+$ T_{regs} or because they are short-lived. Alternatively, the large population of Foxp3$^+$CD25$^-$ICOS$^+$ cells in *Pten*-ΔT_{reg} mice could be an expanded population of effector T_{regs} (eT_R), which have been reported to express low CD25 at the steady state and require ICOS rather than IL-2 for maintenance[36]. Interestingly, inflammation has been shown to drive the proliferation of eT_R and skew cells away from a cT_R phenotype[36]. This finding, along with our data above, suggest that PTEN loss may be crucial in either eT_R differentiation or maintenance.

The functional stability of T_{regs} remains a controversial issue, with several conflicting reports regarding the existence, origin and physiological/pathological role of unstable T_{regs}[31, 32, 34, 37, 38]. Recently, non-T_{reg} cells have been demonstrated to transiently express Foxp3 upon activation, thus generating a small population of 'ex'-Foxp3 cells, which are not 'ex'-T_{regs}[31]. These data indicated that the T_{reg} lineage itself was stable, but "unfaithful" expression of Foxp3 may occur, leading to a population of cells with unstable Foxp3 expression. However, the loss of Foxp3 in *bona fide* T_{regs} occurs in multiple autoimmune settings[32, 38]. Activated by self-antigen, these destabilized T_{regs} acquired effector function and pathogenicity in models of autoimmunity. Consistent with these findings, we find no evidence that PTEN deletion is occurring in non-T_{regs}. We show that 'ex'-Foxp3 cells may also be generated from *bona fide* Foxp3$^+$CD25$^+$ T_{regs} that lack PTEN in a stepwise manner *in vitro*, with loss of CD25 preceding loss of Foxp3. Finally, using lineage reporter mice, we observe that the basal rate of generation of 'ex'-Foxp3 cells from T_{regs} *in vivo* increases approximately three-fold when PTEN is absent.

Despite a normal transcriptional profile compared to PTEN-sufficient T_{regs}, Foxp3$^+$CD25$^-$ cells expressed lower Foxp3 protein than canonical Foxp3$^+$CD25$^+$ T_{regs}, suggesting that the Foxp3$^+$CD25$^-$ T_{reg} population may be enriched for cells with unstable Foxp3 expression. Interestingly, this difference in Foxp3 expression was observed in wild-type T_{regs} as well as

in PTEN-deficient T_{regs}; this association of Foxp3 and CD25 expression has been seen by other groups previously[31–33].

The etiology of lymphoproliferation and autoimmunity in *Pten*-ΔT_{reg} mice may be multifactorial. We provide evidence that PTEN-deficient T_{regs} exhibit lineage instability and can convert into Foxp3^{-} cells. As the TCR repertoire of T_{regs} may be biased to self-antigen recognition[39], this suggests the possibility that disease may be caused by conversion of PTEN-deficient T_{regs} into pathogenic effectors. Although this process of Foxp3 loss in T_{regs} occurs in wild-type mice as well, the absence of disease might be due to the comparative lesser degree of T_{reg} instability and/or the fact that loss of PTEN confers an important survival advantage[10] upon 'ex'-Foxp3 cells. However if 'ex'-Foxp3 cells are pathogenic, they must be "restrainable" by wild-type T_{regs}, as female mice heterozygous for *Foxp3*-Cre do not become ill until their wild-type T_{regs} are largely lost, and *Pten*-iΔT_{reg} remain healthy after tamoxifen injection and resultant loss of Foxp3 in a substantial percentage of T_{regs}. Alternatively, 'ex'-Foxp3 cells that accumulate as a result of PTEN loss may not be pathogenic *per se*, with disease in *Pten*-ΔT_{reg} mice being a consequence of an intrinsic defect in regulation by PTEN-deficient T_{regs}. The inability of *Pten*-ΔT_{reg} mice to resolve EAE in consistent with this possibility.

Activation of signaling through PI3K and mTOR inhibits peripheral T_{reg} induction[14]. One possible mechanism for PI3K control of T_{regs} is via the Foxo1 and Foxo3a (Foxos) transcription factors, which bind to and promote Foxp3 transcription, but are inactivated by PI3K, [17]. Indeed, deletion of Foxos severely inhibits both T_{reg} generation and function *in vivo*, while constitutive nuclear localization of Foxos prevents these defects[18]. Additionally, the maintenance of T_{reg} stability and function by the Neuropilin-1 (Nrp-1)/Semaphorin 4a (Sema4a) signaling axis is due in part to upregulation of PTEN and subsequent nuclear localization of Foxos upon Nrp-1 ligation[40]. Interestingly however, *Pten*-ΔT_{reg} mice develop a different phenotype than animals in which T_{regs} lack Foxo1 expression (as the latter does not affect CD25^{-} expression, nor promote inflammation induced T_{reg} instability) and thus have heightened mTORC2 activation[18]. These disparate phenotypes suggest that multiple factors downstream of PTEN are critical in instructing the T_{reg} lineage.

Modulation of PI3K signaling can alter cellular metabolism[27]. For example, overexpression of PTEN inhibits glycolysis and skews energy generation toward oxidative metabolism[41]. Interestingly, T_{regs} preferentially utilize lipid oxidation for energy, a process characterized by high AMP-activated protein kinase (AMPK) activity[29]. This contrasts with effector T cells, which primarily utilize glycolysis as a means of energy generation[29, 42]. Our data demonstrate that loss of PTEN enhances glycolysis in T_{regs}. The importance of metabolic programs in cellular activation and cell fate decisions is well recognized[43, 44], including a role in determining if cells become *in vitro* induced T_{regs} or induced effectors[29]. Whether alterations in metabolism can affect a pre-existing lineage decision is not known, however the finding that T_{reg} loss of PTEN shifts their metabolic profile suggests that this may be a contributing mechanism by which PTEN deletion destabilizes the T_{reg} lineage, perhaps via an effect on CD25 expression, which precedes loss of Foxp3 during *in vitro* culture.

T cells may express other lipid phosphatases in addition to PTEN that control PI3K signals. One such family, the PH-domain leucine-rich repeat protein phosphatase (PHLPP), is expressed at high levels in murine and human T_{regs}, and is required for optimal iT_{reg} development and T_{reg} function[45]. Our data indicate that despite the expression of additional lipid phosphatases in T_{regs}, PTEN has a non-redundant function in PI3K control and T_{reg} maintenance.

The identification of PI3K as a nodal control point for T_{reg} homeostasis is particularly relevant given the clinical development of PI3K inhibitors for the treatment of autoimmunity or cancer. In the latter arena, the target of PI3K inhibition is the tumor cell itself, although interestingly it was reported recently that inactivation of PI3Kδ in T_{regs} disabled tumor-induced immune suppression and enabled immune-mediated tumor regression in murine models[46]. Whether PI3K blockade has a dominant role in inhibiting regulatory or effector T cell responses is likely to be context and dose-dependent. Our own results showing that high PI3K activity may cripple regulatory responses underscore the complexity of immune system control via this pathway.

Online methods

Mice

Pten$^{fl/fl}$ [9] were bred with *Foxp3*-YFP-*Cre* knock-in mice[47] provided by A. Rudensky (Memorial Sloan Kettering Cancer Center, New York, NY), to generate *Pten*-ΔT_{reg} mice or with *Foxp3*$^{eGFP\text{-}Cre\text{-}ERT2}$ Rosa26-YFP mice[34]– provided by A. Rudensky) to generate mice with tamoxifen inducible loss of PTEN in T_{regs} (Pten-iΔT_{reg} mice). Control animals were either littermates or appropriate age/sex-matched *Pten*$^{+/+}$Foxp3$^{\text{-YFP-Cre}}$ or *Foxp3*$^{eGFP\text{-}Cre\text{-}ERT2}$ Rosa26^{YFP} mice. *Foxp3*$^{GFP\text{-}hCre}$ mice[48] and Rosa26$^{cre\text{-}ER}$ mice[49] have been previously described. Unless otherwise stated, all figures are representative of experiments performed with healthy 6 – 8 week old mice. All mice were housed in specific pathogen-free conditions at Massachusetts General Hospital and the University of California, San Francisco, and all procedures were performed in accordance with protocols approved by each institution's Institutional Animal Care and Use Committee.

Detection of PTEN protein and assessment of the *Pten* genomic locus

Specific deletion of PTEN in Foxp3$^+$ cells at the protein level was assessed via western blotting as described previously[23]. PTEN recombination at the genomic DNA level was performed on highly pure sorted cell populations using previously described primers to specifically detect *Pten*^{flox} and deleted *Pten* alleles[24].

Flow cytometry and cell sorting

Fluorescent anti-CD4 (GK1.5), anti-CD8 (53-6.7), anti-CD24 (30-F1), anti-CD25 (PC-61), anti-CD39 (Duha59), anti-CD44 (IM7), anti-CD62L (MEL-14), anti-CD73 (TY/11.8), anti-CD122 (5H4), anti-CD132 (TUGm2), anti-CXCR3 (CXCR3-173), anti-CXCR5 (L138D7), anti-ICOS (7E.17G9), anti-IFN-γ (XMG1.2), anti-IL-17 (TC11-18H10.1), anti-TCRVβ2 (B20.6) and anti-TCRVβ8 (MR5-2) antibodies were purchased from Biolegend, while anti-PTEN (A2B1), anti-CTLA-4 (UC10-4F10-11), anti-PD-1 (29F.1A12) and anti-CD127 (SB/

199) fluorescent antibodies were purchased from BD Biosciences. Anti-Foxp3 intracellular staining kit and anti-Foxp3 (FJK-16s) antibodies were purchased from eBioscience. For intracellular cytokine staining, cells were restimulated with Leukocyte Activation Cocktail (BD Biosciences) for 5 h at 37°C. For phospho-flow cytometry, cells were serum starved at 37°C for 1 hen activated for 15 minutes with either IL-2 (pSTAT5) or αCD3 and αCD28 (pAkt and pS6). Cells were fixed with paraformaldehyde and permeabilized with methanol. Unconjugated anti-pSTAT5, anti-Akt Ser 473 and anti-S6 antibodies were purchased from Cell Signaling and secondary detection antibody was purchased from Jackson ImmunoResearch. For flow cytometric determination of PTEN, cells were stained with anti-CD25 and anti-CD4 antibodies and then fixed and permeabilized with BD cytofix/cytoperm reagent to preserve endogenous YFP fluorescence. Cells were then stained with an anti-PTEN antibody and run on LSR II flow cytometer. Cells were analyzed on a BD FACSCalibur, BD LSRII or Beckman Coulter Navios and sorted on a BD FACSAria II to over 95% purity; data were analyzed using FlowJo (Tree Star).

T_{reg} culture conditions

T_{regs} were cultured in RPMI medium supplemented with 10% heat-inactivated fetal bovine serum, non-essential amino acids, sodium pyruvate, L-glutamine, HEPES, β-ME with 200 (for *in vitro* induced T_{regs}) or 2,000 IU/ml (nT_{regs}) recombinant human IL-2 (Chiron). *In vitro* induction of Foxp3 from naïve $CD4^+$ T cells was done by stimulation of T cells with plate-bound anti-CD3 (0.1 μg/ml clone 145-2C11 overnight) and anti-CD28 (1 μg/ml clone PV-1 overnight) in the presence of 5 ng/ml TGF-β. PI3K inhibitors were used at the following concentrations: 10 μM LY294002, 100 nM Rapamycin, 100 nM Wortmannin, 1 μM Akt Inhibitor VIII.

Acute deletion of PTEN *in vitro*

T_{regs} from *Pten*$^{fl/+}$ or *Pten*$^{fl/fl}$ mice that also contained Rosa26-CreER were sorted by expression of $CD4^+CD25^+CD62L^+$ and stimulated *in vitro* with anti-CD3 and anti-CD28 coated beads (Dynabeads Mouse T-Activator CD3/CD28, Invitrogen). On day 4 of culture, cells were either treated with 500 nM 4-hydroxytamoxifen (4-OHT, Sigma) or vehicle (ethanol) for the duration of the experiment. CD25 expression was assessed on $CD4^+Foxp3^+$ cells 3 and 10 days after start of treatment.

ELISA

Serum was collected from mice via cardiac puncture for serum Igs and anti-double stranded DNA (anti-dsDNA) antibodies or by serial bleeding for serum creatinine. Immunoglobulin concentrations were detected using the eBioscience Ready-SET-Go! Mouse Ig Isotyping ELISA kit, creatinine concentrations were detected using an ELISA kit from US Biological following the manufacturer's instructions and anti-dsDNA antibodies were detected with an ELISA kit from Alpha Diagnostic as per the manufacturer's instructions.

In vivo BrdU labeling

Mice were injected with 1 mg BrdU (BD Biosciences) i.p. every 12 h for 3 consecutive days. Mice were sacrificed 12 hours after the final injection and cells were stained using a BrdU labeling kit (BD Biosciences) following the manufacturer's instructions.

Induction of EAE

Mice were immunized subcutaneously with MOG 35–55 peptide (UCLA Biopolymers Core) emulsified in Complete Freund's Adjuvant (CFA, Difco) with M. tuberculosis (Difco). Additionally, mice were injected with Pertussis toxin (PT, List Biological Laboratories) i.p. on days 0 and 2 following immunization. Animals were evaluated daily in a blinded manner for signs of disease by the following criteria: 0: no disease; 1: flaccid tail paralysis; 2: hind limb paresis; 3: bilateral hind limb paralysis; 4: fore and hind limb paralysis.

Tamoxifen treatment

Foxp3$^{eGFP\text{-}Cre\text{-}ERT2}$ Rosa26-YFP (i*Foxp3* Cre) and *Pten*$^{fl/fl}$ *Foxp3*$^{eGFP\text{-}Cre\text{-}ERT2}$ Rosa26-YFP (*Pten*-iΔT_{reg}) mice were injected with 2 mg of tamoxifen (Sigma) i.p. for 5 consecutive days to induce Foxp3$^{eGFP\text{-}Cre\text{-}ERT2}$ activity. To simultaneously detect Foxp3 by antibody staining while preserving Rosa-YFP fluorescence, cells were pre-fixed with 2% paraformaldehyde (Electron Microscopy Sciences), fixed and permeabilized using an eBioscience kit and stained intracellularly with an anti-Foxp3 antibody as above.

Histology

Histologic analysis was performed as previously described[23].

Metabolic studies

Extracellular acidification rate (ECAR) and oxygen consumption rate (OCR) were measured by the glycolysis-stress and mito-stress tests, respectively using the XF24 extracellular flux analyzer (Seahorse Bioscience). Briefly, sorted cells were rested for 20–22 hrs in the presence of 1ng/ml IL-2 and 5ng/ml IL-7 followed by the glycolysis-stress test that consisted of seeding 0.5–1 × 10^6 purified cells in glucose free XF Assay media onto a 24 well XF plate coated with cell tak (BD biosciences, CN 354240) followed by sequential addition of glucose (20mM), oligomycin (1μM) and 2-deoxy glucose (20mM). The mito-stress test was performed using glucose (25mM) containing XF assay media and consisted of sequential addition of oligomycin (1μM), FCCP(1.5μM), etomoxir (200μM) followed finally by rotenone (100nM) and antimycin (1μM).

The glycolytic rate was determined by measuring the conversion of 5-^{3}H glucose to tritiated ^3H_2O as described previously[50]. Briefly, 0.5–1.5 × 10^6 purified cells were either unstimulated or stimulated in the presence of plate-bound anti-CD3 (5ug/ml) and anti-CD28 (5ug/ml) and IL-2: 200U/ml. Cells were harvested between 22–24hrs, washed in 1X PBS, resuspended and incubated in Krebs buffer (pH 7.4, 115 mM NaCl, 2 mM KCl, 25mM $NaHCO_3$, 1mM $MgCl_2$, 0.25% BSA) for 30 min at 37°C. Following incubation, 10μCi of radio-labeled 5-^{3}H glucose along with 5 μl 1M cold glucose was added to the cells and

incubated for another additional 1 h at 37°C. Reactions were quenched by addition of 0.5ml of 0.2M HCl. The diffusion chamber setup, the scintillation counting and the calculation of the glycolytic rate were performed as described previously[50]. A cell free sample with 10μCi of radio-labeled 5-^{3}H glucose was included as a negative control and 0.5 μCi of radio-labeled $^{3}H_2O$ was included as a positive control.

Methylation analysis of Foxp3 locus

Genomic DNA from sorted cells was bisulfite converted using the EZ DNA Methylation-Direct kit (Zymo Research) according to the manufacturer's protocol. Methylation-specific PCR primer sequences 5′-TATT TTTTTGGGTTTTGGGATATTA-3′ (forward) and 5′-AACCAACCAACTTCCT ACACTATCTAT-3′ (reverse) were used to amplify intron 1 of Foxp3 (corresponding to Foxp3 CNS2). PCR products were subcloned into pGEM-T Easy vectors (Promega) and sequenced (9–21 sequences per mouse).

Transcriptional profiling

Foxp3^{+}CD25^{+} and Foxp3^{+}CD25^{-} cells were double-sorted to high purity, and RNA was extracted with TRIzol (Life Technologies) according to the manufacturer's instructions. Samples were run in triplicate using a GeneChip Mouse Gene ST 1.0 Array (Affymetrix) and analyzed using GENE-E, GenePattern and Gene Set Enrichment Analysis (Broad Institute).

Supplementary Material

Refer to Web version on PubMed Central for supplementary material.

Acknowledgments

This work was supported by NIH grants R56AI083304 (LAT), R21AI105607 (LAT and JAB), P01HL018646 (LAT) and T32AI007529 (CMB), by a pre-doctoral training grant from the Cancer Research Institute (AH), and by a shared instrumentation grant 1S10RR023440.

References

1. Hori S, Nomura T, Sakaguchi S. Control of regulatory T cell development by the transcription factor Foxp3. Science. 2003; 299:1057–1061. [PubMed: 12522256]
2. Fontenot JD, Gavin MA, Rudensky AY. Foxp3 programs the development and function of CD4+CD25+ regulatory T cells. Nature immunology. 2003; 4:330–336. [PubMed: 12612578]
3. Huynh A, Zhang R, Turka LA. Signals and pathways controlling regulatory T cells. Immunol Rev. 2014; 258:117–131. [PubMed: 24517429]
4. Webster KE, et al. In vivo expansion of T reg cells with IL-2-mAb complexes: induction of resistance to EAE and long-term acceptance of islet allografts without immunosuppression. J Exp Med. 2009; 206:751–760. [PubMed: 19332874]
5. Burchill MA, Yang J, Vogtenhuber C, Blazar BR, Farrar MA. IL-2 receptor beta-dependent STAT5 activation is required for the development of Foxp3+ regulatory T cells. J Immunol. 2007; 178:280–290. [PubMed: 17182565]
6. Ward SG, Ley SC, MacPhee C, Cantrell DA. Regulation of D-3 phosphoinositides during T cell activation via the T cell antigen receptor/CD3 complex and CD2 antigens. Eur J Immunol. 1992; 22:45–49. [PubMed: 1346114]
7. Di Cristofano A, et al. Impaired Fas response and autoimmunity in Pten+/− mice. Science. 1999; 285:2122–2125. [PubMed: 10497129]

8. Stambolic V, et al. Negative regulation of PKB/Akt-dependent cell survival by the tumor suppressor PTEN. Cell. 1998; 95:29–39. [PubMed: 9778245]
9. Suzuki A, et al. T cell-specific loss of Pten leads to defects in central and peripheral tolerance. Immunity. 2001; 14:523–534. [PubMed: 11371355]
10. Liu X, et al. Distinct roles for PTEN in prevention of T cell lymphoma and autoimmunity in mice. J Clin Invest. 2010; 120:2497–2507. [PubMed: 20516645]
11. Bensinger SJ, et al. Distinct IL-2 receptor signaling pattern in CD4+CD25+ regulatory T cells. J Immunol. 2004; 172:5287–5296. [PubMed: 15100267]
12. Zeiser R, et al. Differential impact of mammalian target of rapamycin inhibition on CD4+CD25+Foxp3+ regulatory T cells compared with conventional CD4+ T cells. Blood. 2008; 111:453–462. [PubMed: 17967941]
13. Zanin-Zhorov A, et al. Scaffold protein Disc large homolog 1 is required for T-cell receptor-induced activation of regulatory T-cell function. Proceedings of the National Academy of Sciences of the United States of America. 2012; 109:1625–1630. [PubMed: 22307621]
14. Sauer S, et al. T cell receptor signaling controls Foxp3 expression via PI3K, Akt, and mTOR. Proceedings of the National Academy of Sciences of the United States of America. 2008; 105:7797–7802. [PubMed: 18509048]
15. Zeng H, et al. mTORC1 couples immune signals and metabolic programming to establish T(reg)-cell function. Nature. 2013; 499:485–490. [PubMed: 23812589]
16. Haxhinasto S, Mathis D, Benoist C. The AKT-mTOR axis regulates de novo differentiation of CD4+Foxp3+ cells. J Exp Med. 2008; 205:565–574. [PubMed: 18283119]
17. Ouyang W, et al. Foxo proteins cooperatively control the differentiation of Foxp3+ regulatory T cells. Nat Immunol. 2010; 11:618–627. [PubMed: 20467422]
18. Ouyang W, et al. Novel Foxo1-dependent transcriptional programs control T(reg) cell function. Nature. 2012; 491:554–559. [PubMed: 23135404]
19. Walsh PT, et al. PTEN inhibits IL-2 receptor-mediated expansion of CD4+ CD25+ Tregs. J Clin Invest. 2006; 116:2521–2531. [PubMed: 16917540]
20. Koch MA, et al. The transcription factor T-bet controls regulatory T cell homeostasis and function during type 1 inflammation. Nature immunology. 2009; 10:595–602. [PubMed: 19412181]
21. Li J, et al. PTEN, a putative protein tyrosine phosphatase gene mutated in human brain, breast, and prostate cancer. Science. 1997; 275:1943–1947. [PubMed: 9072974]
22. Xiong H, et al. Characterization of two distinct lymphoproliferative diseases caused by ectopic expression of the Notch ligand DLL4 on T cells. PLoS One. 2013; 8:e84841. [PubMed: 24386421]
23. Zhang R, et al. An obligate cell-intrinsic function for CD28 in Tregs. J Clin Invest. 2013; 123:580–593. [PubMed: 23281398]
24. Backman SA, et al. Deletion of Pten in mouse brain causes seizures, ataxia and defects in soma size resembling Lhermitte-Duclos disease. Nature genetics. 2001; 29:396–403. [PubMed: 11726926]
25. McGeachy MJ, Stephens LA, Anderton SM. Natural recovery and protection from autoimmune encephalomyelitis: contribution of CD4+CD25+ regulatory cells within the central nervous system. J Immunol. 2005; 175:3025–3032. [PubMed: 16116190]
26. Hill JA, et al. Foxp3 transcription-factor-dependent and -independent regulation of the regulatory T cell transcriptional signature. Immunity. 2007; 27:786–800. [PubMed: 18024188]
27. Wang R, Green DR. Metabolic checkpoints in activated T cells. Nat Immunol. 2012; 13:907–915. [PubMed: 22990888]
28. Frauwirth KA, et al. The CD28 signaling pathway regulates glucose metabolism. Immunity. 2002; 16:769–777. [PubMed: 12121659]
29. Michalek RD, et al. Cutting edge: distinct glycolytic and lipid oxidative metabolic programs are essential for effector and regulatory CD4+ T cell subsets. J Immunol. 2011; 186:3299–3303. [PubMed: 21317389]
30. Polansky JK, et al. DNA methylation controls Foxp3 gene expression. European journal of immunology. 2008; 38:1654–1663. [PubMed: 18493985]

31. Miyao T, et al. Plasticity of Foxp3(+) T cells reflects promiscuous Foxp3 expression in conventional T cells but not reprogramming of regulatory T cells. Immunity. 2012; 36:262–275. [PubMed: 22326580]
32. Komatsu N, et al. Pathogenic conversion of Foxp3(+) T cells into TH17 cells in autoimmune arthritis. Nature medicine. 2014; 20:62–68.
33. Wan YY, Flavell RA. Regulatory T-cell functions are subverted and converted owing to attenuated Foxp3 expression. Nature. 2007; 445:766–770. [PubMed: 17220876]
34. Rubtsov YP, et al. Stability of the regulatory T cell lineage in vivo. Science. 2010; 329:1667–1671. [PubMed: 20929851]
35. Shrestha S, et al. The Pten-mTORC2 axis coordinates Treg stability and control of TH1 and TFH cell flexibility. Nature Immunology. (In press).
36. Smigiel KS, et al. CCR7 provides localized access to IL-2 and defines homeostatically distinct regulatory T cell subsets. The Journal of experimental medicine. 2014; 211:121–136. [PubMed: 24378538]
37. Zhou X, et al. Instability of the transcription factor Foxp3 leads to the generation of pathogenic memory T cells in vivo. Nat Immunol. 2009; 10:1000–1007. [PubMed: 19633673]
38. Bailey-Bucktrout SL, et al. Self-antigen-driven activation induces instability of regulatory T cells during an inflammatory autoimmune response. Immunity. 2013; 39:949–962. [PubMed: 24238343]
39. Hsieh CS, Zheng Y, Liang Y, Fontenot JD, Rudensky AY. An intersection between the self-reactive regulatory and nonregulatory T cell receptor repertoires. Nat Immunol. 2006; 7:401–410. [PubMed: 16532000]
40. Delgoffe GM, et al. Stability and function of regulatory T cells is maintained by a neuropilin-1-semaphorin-4a axis. Nature. 2013; 501:252–256. [PubMed: 23913274]
41. Garcia-Cao I, et al. Systemic elevation of PTEN induces a tumor-suppressive metabolic state. Cell. 2012; 149:49–62. [PubMed: 22401813]
42. Gwinn DM, et al. AMPK phosphorylation of raptor mediates a metabolic checkpoint. Molecular cell. 2008; 30:214–226. [PubMed: 18439900]
43. Delgoffe GM, et al. The mTOR kinase differentially regulates effector and regulatory T cell lineage commitment. Immunity. 2009; 30:832–844. [PubMed: 19538929]
44. Dang EV, et al. Control of T(H)17/T(reg) balance by hypoxia-inducible factor 1. Cell. 2011; 146:772–784. [PubMed: 21871655]
45. Patterson SJ, et al. Cutting edge: PHLPP regulates the development, function, and molecular signaling pathways of regulatory T cells. J Immunol. 2011; 186:5533–5537. [PubMed: 21498666]
46. Ali K, et al. Inactivation of PI(3)K p110delta breaks regulatory T-cell-mediated immune tolerance to cancer. Nature. 2014; 509:407–411. [PubMed: 24848039]
47. Rubtsov YP, et al. Regulatory T cell-derived interleukin-10 limits inflammation at environmental interfaces. Immunity. 2008; 28:546–558. [PubMed: 18387831]
48. Zhou X, et al. Selective miRNA disruption in T reg cells leads to uncontrolled autoimmunity. J Exp Med. 2008; 205:1983–1991. [PubMed: 18725525]
49. Badea TC, Wang Y, Nathans J. A noninvasive genetic/pharmacologic strategy for visualizing cell morphology and clonal relationships in the mouse. J Neurosci. 2003; 23:2314–2322. [PubMed: 12657690]
50. Vander Heiden MG, et al. Growth factors can influence cell growth and survival through effects on glucose metabolism. Mol Cell Biol. 2001; 21:5899–5912. [PubMed: 11486029]

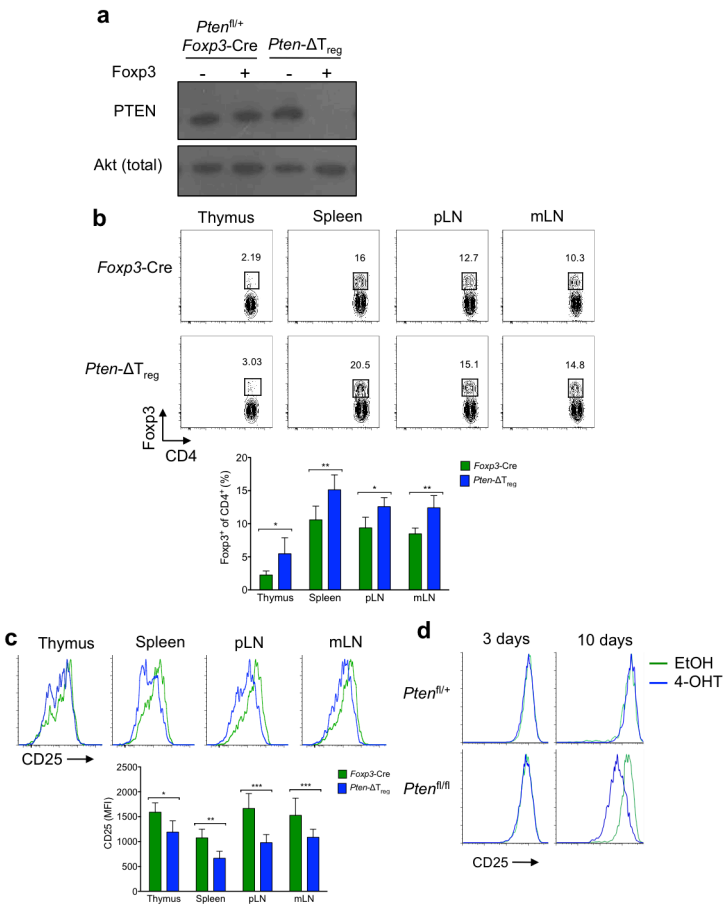

Figure 1.

Characterization of *Pten*-ΔT_{reg} mice. (**a**) Foxp3$^+$ and Foxp3$^-$ cells were sort purified from the indicated mice and cell populations were analyzed by immunoblotting for PTEN and total Akt. (**b**) Analysis of CD4 and Foxp3 in cells isolated from the indicated tissues (pLN, peripheral lymph node; mLN, mesenteric lymph node). n = 10, representative of 10 experiments; *p < 0.001, **p < 0.0001 by two-way ANOVA. (**c**) Expression of CD25 on Foxp3$^+$ cells isolated from thymus, spleen, pLN and mLN from *Pten*-ΔT_{reg} and wild-type mice. n = 10, representative of 10 experiments; *p < 0.05, **p < 0.01, ***p < 0.001 by two-way ANOVA. (**d**) CD4$^+$CD25$^+$CD62L$^+$ sorted T_{regs} from *Pten*$^{fl/+}$ or *Pten*$^{fl/fl}$ Rosa26-CreER mice were cultured for the indicated times *in vitro* in the presence of 4-OH tamoxifen (4-OHT) to induce Cre-mediated excision of *Pten* and assessed for CD25 expression. Representative of 2 experiments. All error bars shown are mean ± SD.

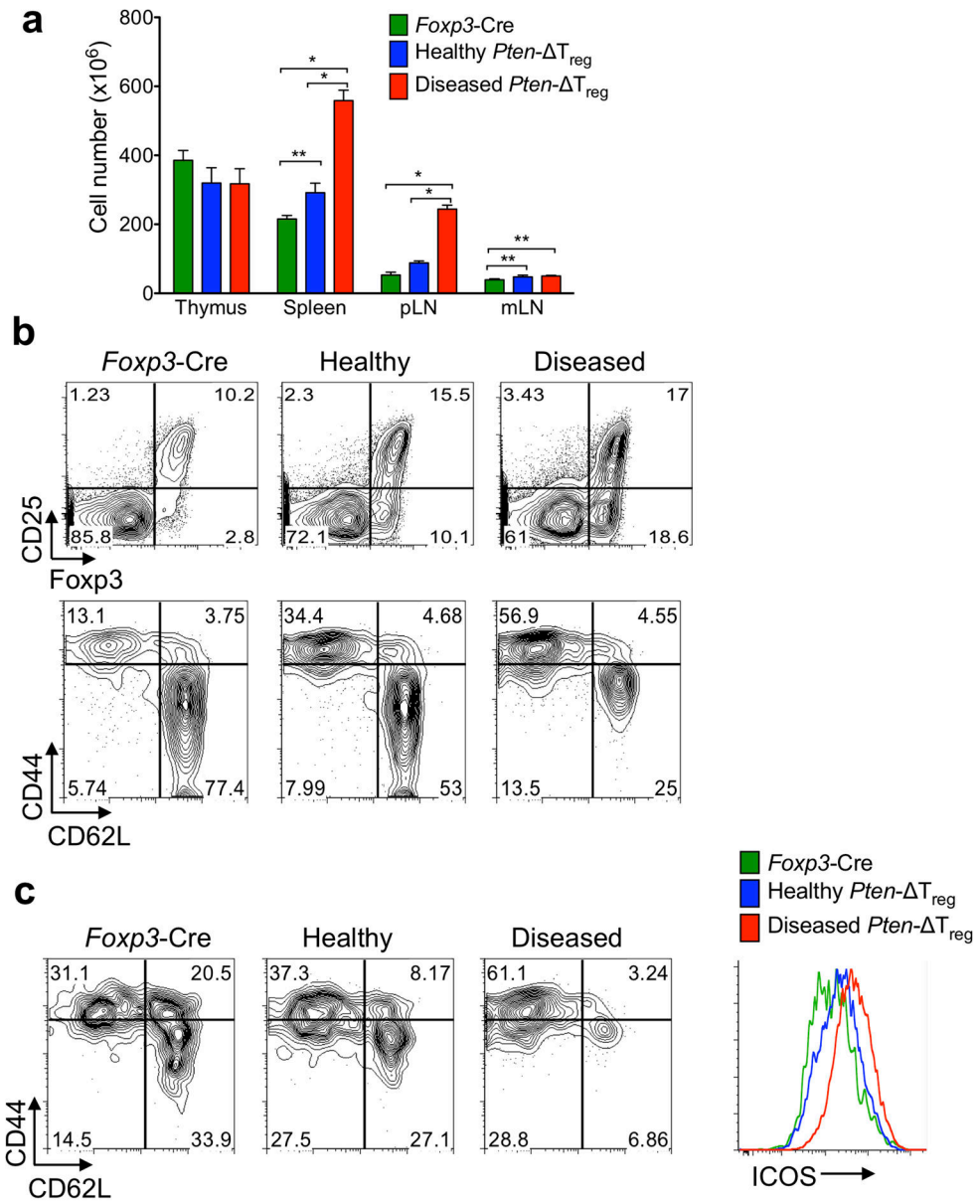

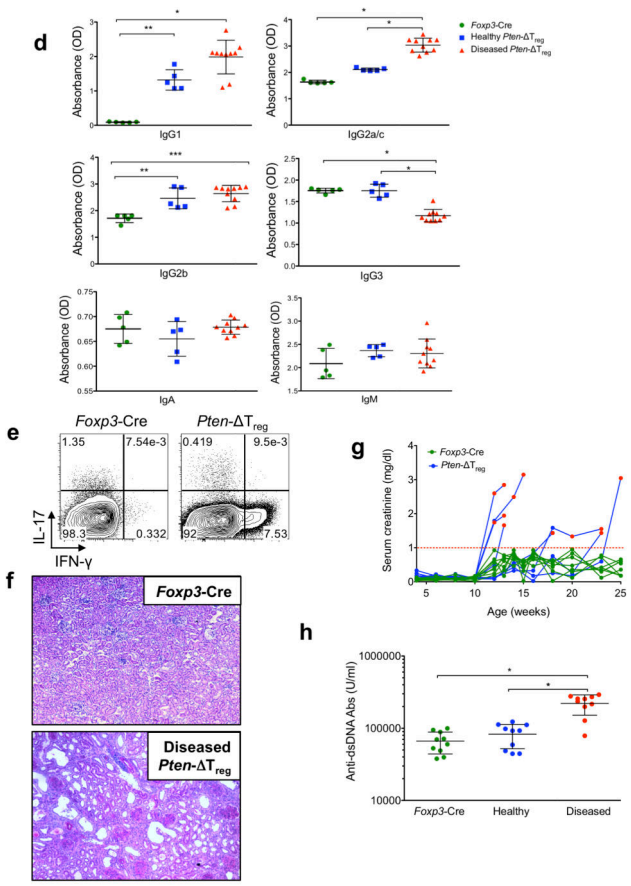

Figure 2.

Pten-ΔT_{reg} mice develop spontaneous systemic lymphoproliferative disease with age. (**a**) (Left) Cell numbers from the indicated tissues of *Foxp3*-Cre control mice, healthy appearing *Pten*-ΔT_{reg} mice, and diseased *Pten*-ΔT_{reg} mice (as assessed by gross lymphadenopathy, typical age 15 – 18 weeks). $n = 3$ for diseased *Pten*-ΔT_{reg} or 5 for other groups; representative of 5 experiments; $*p < 0.0001$, $**p < 0.01$ by two-way ANOVA. (**b**) Flow cytometric analysis of $CD4^+$ cells (top) and $CD4^+Foxp3^-$ cells (bottom) from spleen of wild-type mice, *Pten*-ΔT_{reg} mice, and diseased *Pten*-ΔT_{reg} mice. Representative of 10 experiments. (**c**) $Foxp3^+$ T_{regs} were isolated from wild-type, *Pten*-ΔT_{reg} and diseased *Pten*-ΔT_{reg} mice and analyzed for expression of CD44, CD62L and ICOS. Representative of 10 experiments. (**d**) Serum IgG1, IgG3a/c, IgG2b, IgG3, IgA and IgM concentrationss from the three groups of mice as defined above. $n = 10$ for diseased *Pten*-ΔT_{reg} and 5 for other groups, representative of 3 experiments; $*p < 0.0001$, $**p < 0.001$, $***p = 0.0001$ by one-way ANOVA. (**e**) $CD4^+$ cells from lymph nodes of control mice and diseased *Pten*-ΔT_{reg} mice were isolated, restimulated *ex vivo* and stained for IFN-γ and IL-17, representative of 5 experiments. (**f**) Hematoxylin and eosin staining of renal tissue from a representative wild-type (top) and *Pten*-ΔT_{reg} mouse (bottom); 10x magnification. (**g**) Serum creatinine concentrations in *Pten*-ΔT_{reg} mice with age. $n = 8$, representative of 2 experiments. Red symbols indicate age at which visible lymphadenopathy occurred; red line indicates the level at which kidney failure is diagnosed in mice. (**h**) Anti-double stranded DNA antibody

concentrations in *Pten*-ΔT_{reg} mice. $n = 10$, representative of 2 experiments; $^*p < 0.0001$ by one-way ANOVA. All error bars shown are mean ± SD.

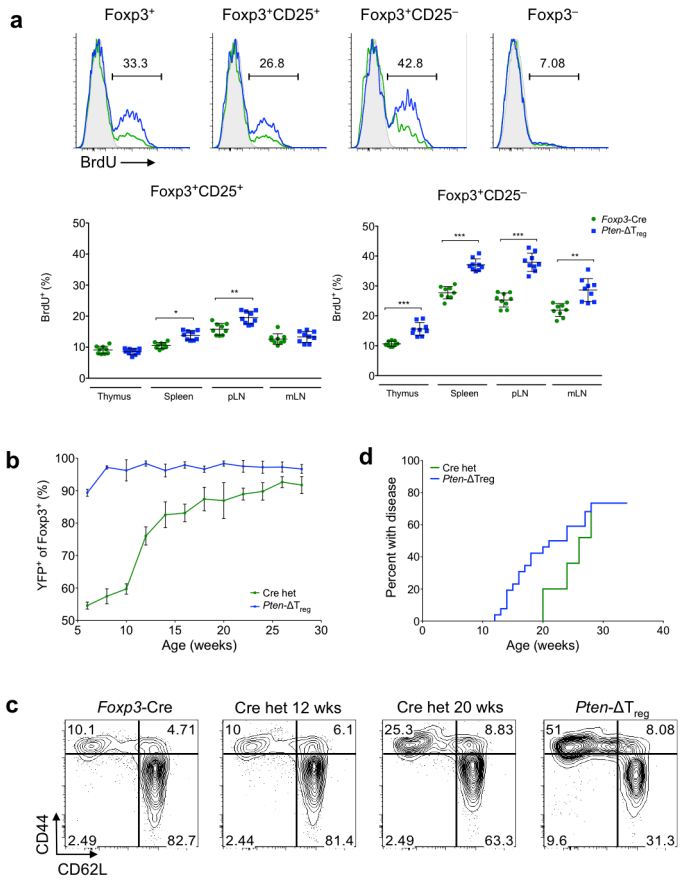

Figure 3.

Expansion of PTEN-deficient T_{regs} *in vivo*. (**a**) Wild-type and *Pten*-ΔT_{reg} mice were injected i.p. with BrdU every 12 h for 3 consecutive days. Cells were isolated from thymus, spleen, pLN and mLN and assessed for BrdU incorporation. $n = 9$, representative of 4 experiments; $*p < 0.001$, $**p < 0.002$, $***p < 0.0001$ by t-test. (**b**) Female *Pten*$^{fl/fl}$ mice were bred to express one allele of *Foxp3*-Cre (Cre heterozygous mice) and followed over time along with female *Pten*-ΔT_{reg} mice (homozygous for *Foxp3*-Cre). $n = 20$. (**c**) Flow cytometric analysis of peripheral blood CD4$^+$Foxp3$^-$ T cells from mice as in panel **b** plus a wild-type *Foxp3*-Cre control mouse. (**d**) Aged *Pten*$^{fl/fl}$ Cre heterozygous female mice develop disease similar to *Pten*-ΔT_{reg} mice with delayed onset, $n = 20$ (Cre het) or 35 (*Pten*-ΔT_{reg}). All error bars shown are mean ± SD.

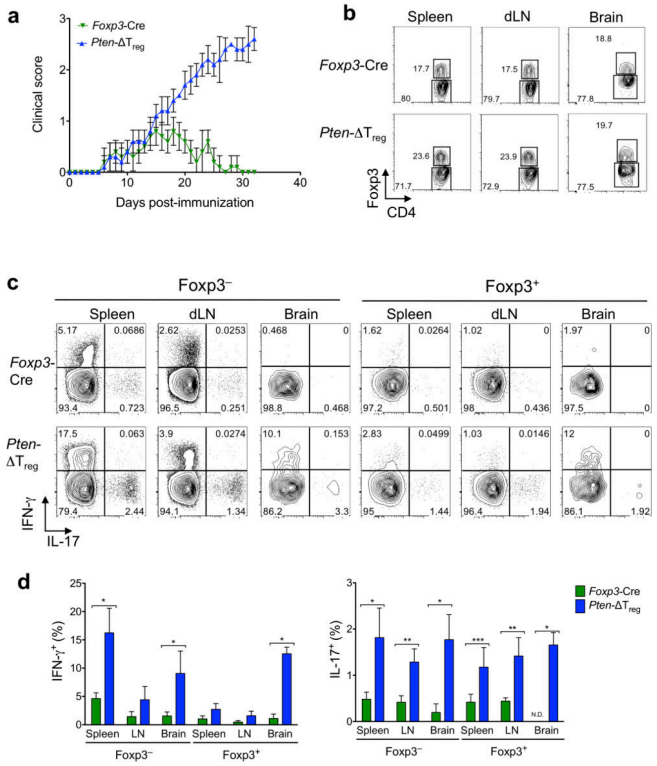

Figure 4.

Loss of PTEN prevents the ability of T_{regs} to resolve autoimmune inflammation. (**a**) Wild-type and *Pten*-ΔT_{reg} mice were immunized s.c. with myelin oligodendrocyte peptide emulsified in complete Freund's adjuvant (CFA) to induce experimental autoimmune encephalomyelitis (EAE), and clinical disease severity was monitored for 35 days post-immunization. $n = 10$, representative of 3 experiments; $p < 0.0001$ by two-way ANOVA. (**b**) Representative flow cytometric analysis for CD4 and Foxp3 in the spleen, draining lymph nodes and brain of mice in panel **a** at day 35. (**c**) T cells as in panel **b** were restimulated *ex vivo* and assessed for production of IFN-γ and IL-17. Left set of panels are gated on $CD4^+Foxp3^-$ cells and the right set of panels are gated on $CD4^+Foxp3^+$ cells. $n = 5$, representative of 3 experiments. (**d**) Compilation of data from the experiments in **c**. N.D. = not detected; $*p < 0.0001$, $**p < 0.001$, $***p < 0.01$ by two-way ANOVA. All error bars shown are mean ± SD.

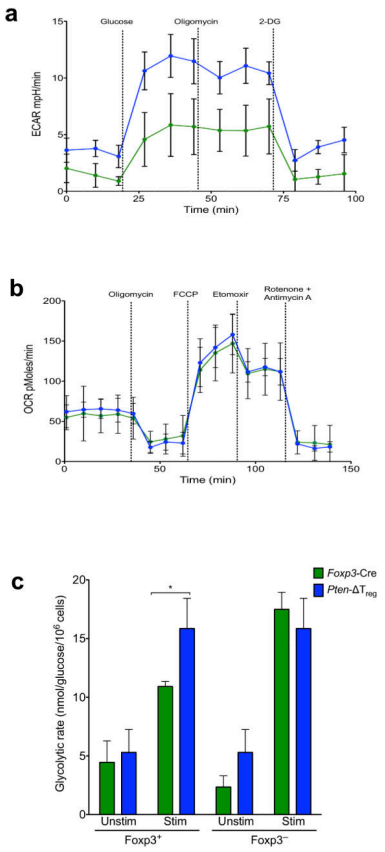

Figure 5.

PTEN deficiency skews T_{reg} metabolism toward glycolysis. (**a,b**) T_{regs} from *Pten*-ΔT_{reg} and wild-type mice were purified and subjected to a glycolysis stress (**a**) or mito-stress test (**b**) to assess the bioenergetic profile of these cells. $n = 3$ samples per group, representative of 2 experiments. (**c**) The indicated populations of cells were isolated from *Pten*-ΔT_{reg} or wild-type mice, stimulated and treated with [3-^{3}H] glucose to measure the generation of ^3H_2O as an indicator of the glycolytic rate of cells. $n = 4$, representative of 3 experiments; $*p < 0.01$ by two-way ANOVA. All error bars shown are mean ± SD.

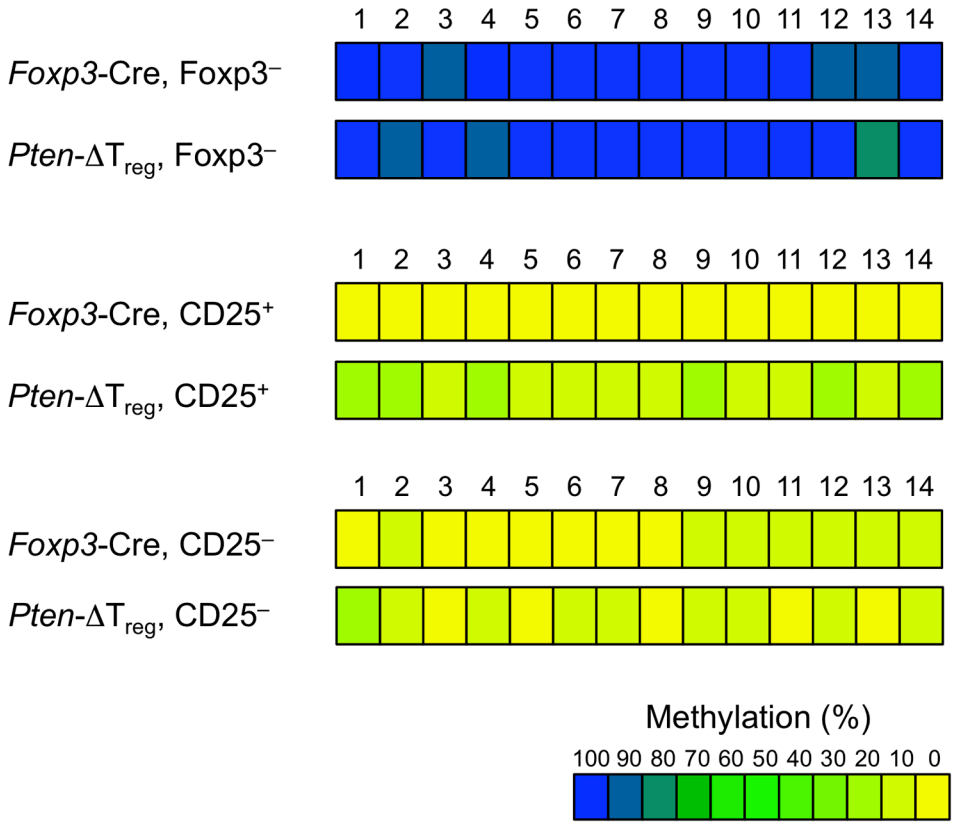

Figure 6.

TSDR methylation analysis. Methylation status of CpG motifs of the Foxp3 locus was assessed by bisulfite sequencing of the indicated populations of sorted cells (data were averaged from 4 – 5 mice per group and > 76 total sequences per group).

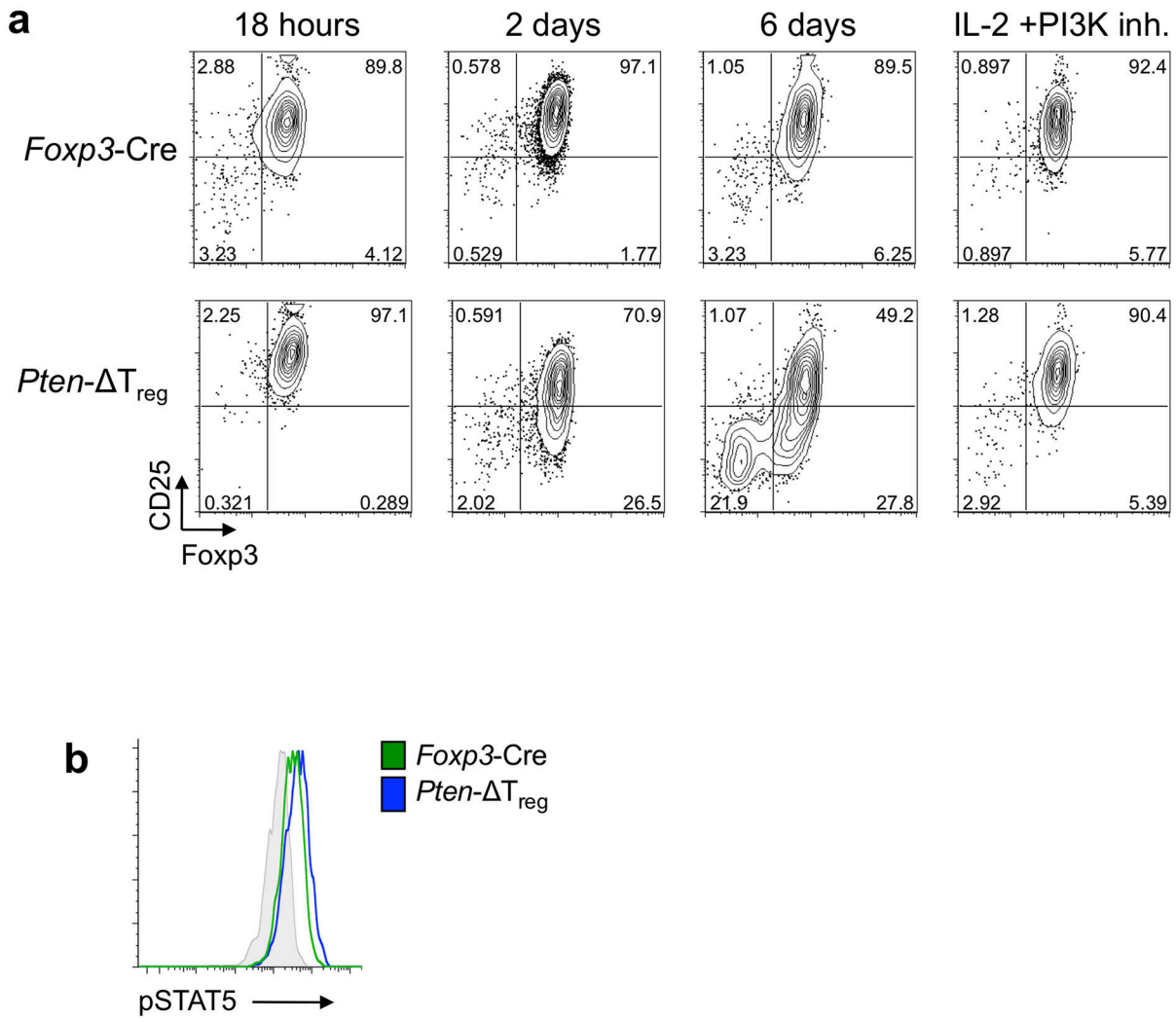

Figure 7.

PTEN deletion leads to T_{reg} instability *in vitro*. (**a**) $CD4^+Foxp3^+CD25^+$ iT_{regs} from *Pten*$^{fl/fl}$ *Foxp3*$^{GFP\text{-}hCre}$ mice with indicated genotypes were sorted and cultured in the presence of IL-2 with or without the PI3K inhibitor (10 μM LY294002) for 6 d and expression of Foxp3 and CD25 was monitored at indicated times. Representative of 3 experiments. (**b**) $Foxp3^+$ cells were isolated from wild-type and *Pten*-ΔT_{reg} mice, serum starved for 1 h and stimulated for 30 min in the presence of 200 IU/ml hIL-2. Cells were then immediately fixed, permeabilized and assessed for pSTAT5 levels by phospho-flow cytometry. Grey = isotype control. Representative of 3 experiments.

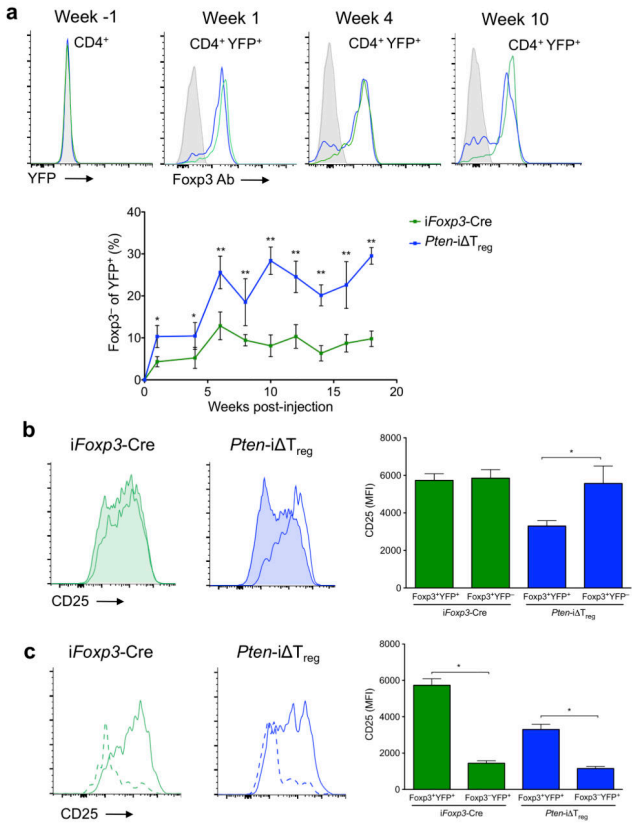

Figure 8.

PTEN deletion leads to T_{reg} instability *in vivo*. Control and *Pten*-iΔT_{reg} mice were treated with a 5 d course of tamoxifen as per Materials and Methods. Peripheral blood was assessed at the indicated time points. (**a**) Detection and quantification of 'ex'-Foxp3 cells. All plots are gated on $CD4^+YFP^+$ cells, except Week -1, which is gated on total $CD4^+$ cells. $n = 5$, representative of 3 experiments; $*p < 0.05$, $**p < 0.0001$ by two-way ANOVA. **(b)** Expression of CD25 on $Foxp3^+$ cells. CD25 staining of $Foxp3^+YFP^+$ T_{regs} (unshaded) and $Foxp3^+YFP^-$ (shaded) unlabeled T_{regs} from a representative animal at week 20 as per panel **a**. $n = 5$, representative of 3 experiments, $*p < 0.0001$ by two-way ANOVA. **(c)** Expression of CD25 on 'ex'-Foxp3 cells. CD25 staining of $Foxp3^-YFP^+$ (dashed) and $Foxp3^+YFP^+$ (solid) cells for the animal shown in panel **b**. $n = 5$, representative of 3 experiments; $*p < 0.0001$ by two-way ANOVA. All error bars are mean ± SD.